



ELSEVIER

Biophysical Chemistry 75 (1998) 213–227

Biophysical  
Chemistry

## Oligomerization and phase separation in globular protein solutions

Neer Asherie<sup>a</sup>, Jayanti Pande<sup>a</sup>, Aleksey Lomakin<sup>a</sup>, Olutayo Ogun<sup>a</sup>,  
Stacy R.A. Hanson<sup>b</sup>, Jean B. Smith<sup>b</sup>, George B. Benedek<sup>a,\*</sup>

<sup>a</sup> *Department of Physics and Center for Materials Science and Engineering, Rm 13-2005, Massachusetts Institute of Technology, 77 Massachusetts Avenue, Cambridge, MA 02139-4307, USA*

<sup>b</sup> *Department of Chemistry, University of Nebraska, Lincoln, NE 68588-0304, USA*

Received 31 August 1998; accepted 24 September 1998

---

### Abstract

We have chemically crosslinked a globular protein,  $\gamma_{\text{IIIb}}$ -crystallin, to produce a system of well-defined oligomers: monomers, dimers, trimers and a mixture of higher  $n$ -mers. Gel electrophoresis, size exclusion chromatography, quasielastic light scattering spectroscopy, and electrospray ionization mass spectrometry were used to characterize the oligomers formed. The liquid–liquid phase separation boundaries of the various oligomers were measured. We find that at a given concentration the phase separation temperature strongly increases with the molecular weight of the oligomers. This phase behavior is very similar to previous findings for  $\gamma_{\text{II}}$ -crystallin, for which oxidation-induced oligomerization is accompanied by an increase in the phase separation temperature. These findings imply that for phase separation, the detailed changes of the surface properties of the proteins are less important than the purely steric effects of oligomerization. © 1998 Elsevier Science B.V. All rights reserved.

*Keywords:* Liquid–liquid phase separation;  $\gamma$ -Crystallins; Oligomerization; Crosslinking

---

\* Corresponding author. Tel.: +1 617 2534828; fax: +1 617 2252585; e-mail: gbb@mit.edu

*Abbreviations:* BMH, bismaleimido-hexane; CAT-HPLC, cation exchange high performance liquid chromatography; DTNB, 5,5'-dithiobis(2-nitrobenzoic acid); DTT, dithiothreitol; ESIMS, electrospray ionization mass spectrometry; GU, guanidine hydrochloride; HPLC, high performance liquid chromatography; NMR, nuclear magnetic resonance; PTC, phenylisothiocyanate; QLS, quasielastic light scattering spectroscopy; SX-HPLC, size exclusion high performance liquid chromatography

0301-4622/98/\$ - see front matter © 1998 Elsevier Science B.V. All rights reserved.

PII S0301-4622(98)00208-7

## 1. Introduction

Aggregation, a common phenomenon in protein solutions [1], frequently alters the normal biochemical and biophysical properties of proteins. For example, aggregation of proteins is responsible for the formation of inclusion bodies in bacterial cells [2], the loss of protein stability in drug delivery [3] and the pathology observed in protein condensation diseases [4]. Aggregation in biological systems is governed by both specific and non-specific interactions. The non-specific interactions lead to amorphous aggregates which often cannot be obtained reproducibly *in vitro* [5]. Consequently, it is difficult to systematically study the effects of aggregation on the physical and chemical properties of protein solutions. In particular, it is not easy to understand to what extent the properties of aggregated protein solutions result from the aggregation itself, and to what extent do the properties depend on the specific chemical structure of the aggregates. It is therefore important to develop model systems in which well-defined aggregates can be produced in a controlled fashion.

Aggregation is driven by attractive interactions between proteins. Attractive interactions also drive the liquid–liquid phase separation [6] and crystallization [7] of protein solutions. Since aggregation and phase separation are both facilitated by attractive interactions, they are often observed simultaneously and indeed compete with one another in protein solutions. For example, one of the major obstacles in the crystallization of proteins is the formation of amorphous aggregates [8]. Aggregation also interferes with the liquid–liquid phase separation of protein. This poses a problem in aqueous phase separation technology, where liquid–liquid phase separation is used to concentrate and purify proteins [9].

Although aggregation and phase separation in protein solutions have been studied separately by many authors [10–15], there are few works which examine quantitatively the effect of aggregates on the phase separation of protein solutions. This is partly because there are few protein systems for which full phase diagrams have been determined. One family of proteins in which crystallization,

liquid–liquid phase separation and aggregation have all been observed are the  $\gamma$ -crystallins, a homologous family of monomeric proteins found in the mammalian eye lens [16–20]. The phase behavior of these proteins has been implicated in the opacification of the eye lens which occurs in cataract ([4] and references therein). Aggregates of  $\gamma$ -crystallins have been isolated from cataractous lenses [16,21], and work in our group has shown that the phenomenon of cold cataract (in which animal lenses cloud when their temperature is lowered) is due primarily to the liquid–liquid phase separation of the  $\gamma$ -crystallins [22]. However, it was only recently observed that the aggregation of the  $\gamma$ -crystallins can directly affect the location of the liquid–liquid phase separation boundary (the coexistence curve) [23].

The recent work of Pande et al. [23] has shown that, under oxidative conditions, the liquid–liquid phase separation temperature of a solution of  $\gamma_{II}$ - ( $\gamma$ B-) crystallin increases with time. This increase was found to be due to the formation of a new protein species,  $\gamma_{III}$ -crystallin. When isolated,  $\gamma_{III}$  was found to be a composite species consisting of an intermolecular disulphide-crosslinked dimer and loosely associated oligomers [23,24]. These findings clearly demonstrated that aggregation has a significant effect on the liquid–liquid phase boundary of a protein solution. However, due to the inherent variability of the aggregation process (e.g. the variation in the proportion of oligomers to dimers) and the high phase separation temperatures (above 45°C), it was not possible to use  $\gamma_{III}$  for a detailed study of the effects of aggregation on liquid–liquid phase separation. We therefore developed a model system of well-defined oligomers which was then used to investigate the effect of aggregation on the location of the coexistence curve.

We report here our work on the liquid–liquid phase separation of oligomers of  $\gamma_{IIb}$ - ( $\gamma$ D-) crystallin. These oligomers were made by chemically crosslinking the native protein. We chose the protein  $\gamma_{IIb}$ -crystallin as our model system since its critical temperature  $T_c$  is approximately 5°C [19], and therefore the protein solution can be handled at room temperature without under-

going phase separation. Also, unlike  $\gamma_{II}$ ,  $\gamma_{IIIb}$  does not form dimers spontaneously by oxidation under the same solution conditions (Pande et al., unpublished data). This allows us to obtain repeatedly the same proportions of the various oligomers of  $\gamma_{IIIb}$  and to separate the oligomers into monomer, dimer, trimer and higher  $n$ -mer fractions. Work in this laboratory and elsewhere has shown that the thiol groups of the  $\gamma$ -crystallins are accessible to chemical modifications [24–28]. One such modifier, the monofunctional reagent *N*-ethylmaleimide, has been shown to specifically modify the thiol groups of the  $\gamma$ -crystallins [26]. We therefore chose a bismaleimido-hexane, a bifunctional analog of *N*-ethylmaleimide, to form oligomers of  $\gamma_{IIIb}$ . With this reagent we were able to produce the large quantities of protein oligomers necessary for phase separation studies.

## 2. Materials and methods

### 2.1. Preparation of pure $\gamma_{IIIb}$ -crystallin solutions

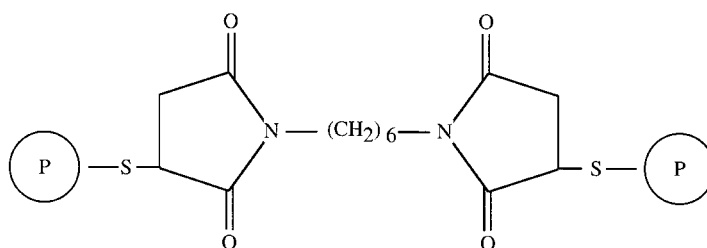
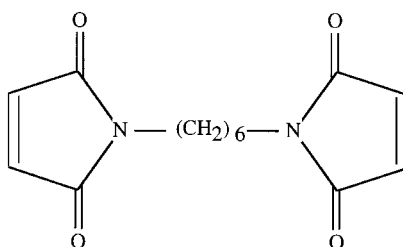
The  $\gamma_{IIIb}$ -crystallin used in our study was isolated from 1- to 6-week-old calf lenses, obtained by overnight express from Antech (Tyler, TX). The monomeric  $\gamma$ -crystallin fraction was isolated from the soluble protein fraction by size exclusion chromatography on Sephadex G-75, as described by Thomson et al. [17]. Native  $\gamma$ -crystallin so obtained was further fractionated into  $\gamma_I$ ,  $\gamma_S$ ,  $\gamma_{II}$ ,  $\gamma_{III}$  and  $\gamma_{IV}$  by cation exchange chromatography on Sulfopropyl Sephadex C-50, according to Thomson et al. [17]. Anion exchange chromatography at pH 8.8 on diethylaminoethyl-Sephadex was used to fractionate  $\gamma_{III}$  into  $\gamma_{IIIa}$  and  $\gamma_{IIIb}$  as described by Broide et al. [19]. Native  $\gamma_{III}$  consists of  $\approx 60\%$   $\gamma_{IIIb}$  and  $\approx 40\%$   $\gamma_{IIIa}$  by weight. Immediately after elution, the pure  $\gamma_{IIIb}$  fraction was transferred into 275 mM sodium acetate buffer, pH 4.8, to minimize the oxidation of sulfhydryl groups that occurs more quickly at the higher pH. We designate this  $\gamma_{IIIb}$  fraction at low pH as the native protein sample. The purity of the native sample was at least 98%, based on both CAT-HPLC, and SX-HPLC. These methods are described in Section 2.3.

The purified  $\gamma_{IIIb}$  fraction was dialyzed exhaustively into 100 mM sodium phosphate buffer (ionic strength 240 mM, pH 7.1), which contained sodium azide (0.02%). The concentrations of the pure monomeric  $\gamma_{IIIb}$  samples were determined by UV absorption at 280 nm, as described by Broide et al. [19], using the extinction coefficient  $E_{280}^{0.1\%,1\text{cm}} = 2.11$ . We have also used this value of the extinction coefficient to determine the concentrations of the oligomer samples. With this value we find that the total mass of the protein after the crosslinking reaction is the same as the starting mass to within 5%. The protein volume fraction  $\phi$  was obtained from the concentration  $C$  (in mg/ml) by using the expression  $\phi = \bar{v}C$ . For most globular proteins, including oligomeric ones, the value of the specific volume  $\bar{v}$  is approximately,  $\bar{v} = 0.71 \text{ cm}^3/\text{g}$  [29]. We therefore use this value for the control and oligomer samples of  $\gamma_{IIIb}$ . Precautions were taken to obtain aggregate-free and crystal-free solutions [19,20,30].

### 2.2. Production of oligomers

The oligomers of  $\gamma_{IIIb}$ -crystallin were produced by crosslinking the native monomeric protein with the homobifunctional reagent bismaleimido-hexane (BMH; Pierce Chemical Company, Rockford, IL) [31–33]. This reagent is a member of a homologous series of the form  $(\text{C}_4\text{H}_2\text{O}_2\text{N})_2(\text{CH}_2)_n$ , with  $n = 6$  for BMH [34]. At neutral pH, BMH reacts specifically with thiol groups [34]. The structure of BMH and the expected structure of a protein dimer are shown in Fig. 1. The reagent is insoluble in water, and has been added to aqueous protein solutions in the solid form [35]. For our reactions the mass of BMH used was such that the mole ratio of protein to BMH was unity. Typically 5 ml of  $\gamma_{IIIb}$  at 30–40 mg/ml (in phosphate buffer, pH 7.1) were added to the appropriate amount of dry, solid BMH (approx. 2–3 mg). The solution was reacted at room temperature for 3 h while being stirred constantly. Since BMH is insoluble in water the solution appeared slightly cloudy even at the beginning of the reaction. By the end of the reaction the cloudiness had increased, presumably due to the formation of large aggregates of proteins.

Bismaleimidohexane (BMH)



Schematic structure of dimer

Fig. 1. The expected reaction of bismaleimidohexane (BMH) with thiol groups on a protein, schematically shown as P. The final product is the expected structure of the dimer.

The reaction was not quenched, but at the end of 3 h the sample was centrifuged for 30 min at 10 000 rev./min. The supernatant was removed and filtered (0.22  $\mu\text{m}$  filter). The resulting solution was clear. The composition of this solution was determined by SX-HPLC on a Superdex 200HR column (see Section 2.3.2). Typically, the solution contained 30% monomers, 60% dimers and 10% higher oligomers (Fig. 2). Since some of the monomer will have reacted with the crosslinker, this fraction will no longer be native-like. We will refer to this monomer fraction as the 'post-reaction monomer' (pr-monomer) to distinguish it from the native monomer protein. To collect the large amounts of material needed for phase separation studies, the individual oligomers (for simplicity, the term oligomer includes the pr-monomer and the dimer fractions) were isolated by low pressure size exclusion chro-

matography on an XK26/70 Superdex-75 column (Pharmacia Biotech, Piscataway, NJ) at a flow rate of 1 ml/min, with 100 mM sodium phosphate buffer containing sodium azide (0.02%). This allowed not only for a large scale separation, but also for a better resolution between monomers, dimers and trimers than was possible with the Superdex 200HR column. The final yields of the oligomers (as a percentage of the initial amount of protein) after the low pressure Superdex-75 separation were  $\sim$  15% pr-monomer, 30% dimer and 3% trimer. These fractions were each at least 99% pure as determined by SX-HPLC. The good resolution of the low pressure column enabled us also to collect a mixture of higher  $n$ -mers (trimers, tetramers and pentamers). A control  $\gamma_{\text{IIIb}}$  sample was prepared exactly as the oligomer samples except that no crosslinker was added to the solution.

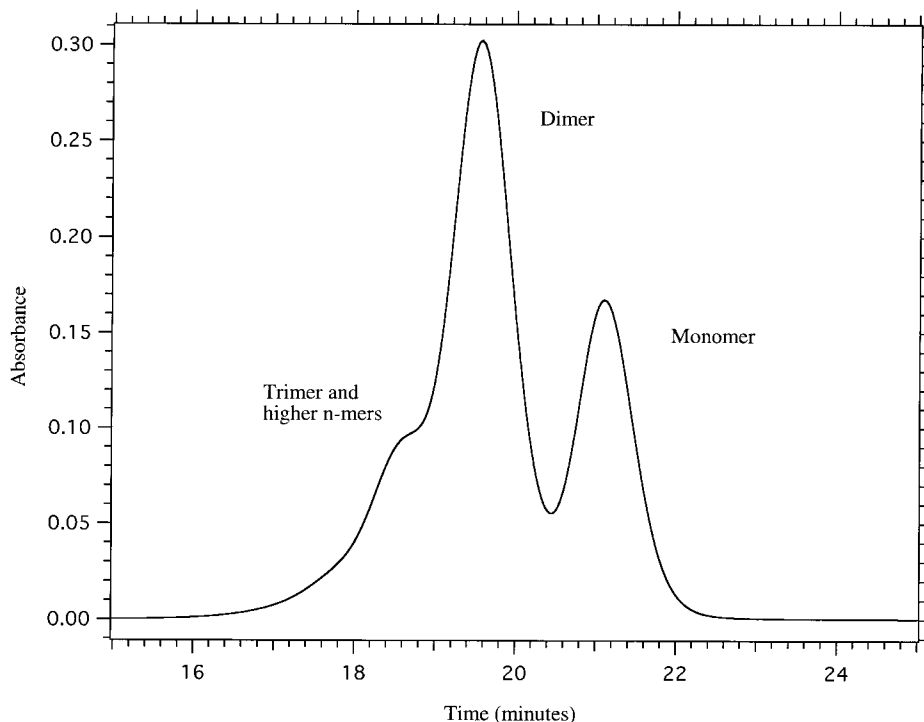


Fig. 2. Size exclusion chromatography results (on a Superdex 200HR column) for the crosslinked protein after a 3 h reaction. The absorbance at 280 nm is shown as function of retention time in min.

In the next section we describe the characterization of the oligomers we obtained.

### 2.3. Characterization of oligomers

#### 2.3.1. Gel electrophoresis

SDS/PAGE was carried out on 12% gels in the absence of urea with a Mini-Protean II electrophoresis system (Bio-Rad). Conditions were as described elsewhere [36,37]. Gels were run with and without DTT. This reagent reduces disulphide crosslinks and has been shown to dissociate  $\gamma_{III}$  completely into monomers [23].

#### 2.3.2. Size exclusion HPLC

SX-HPLC was carried out according to Friberg et al. [24] with a Superdex 200HR column from Pharmacia Biotech at a flow rate of 1 ml/min. The buffer used was 100 mM sodium phosphate (pH 7.1) with 0.02% sodium azide.

#### 2.3.3. Thiol content

The thiol content of the control and oligomer samples of  $\gamma_{IIIb}$  were determined by the DTNB assay, described by Truscott and Martin [38]. All solutions were degassed and kept under argon during measurements. The number of free thiols was estimated using the extinction coefficient  $\epsilon_{412} = 13.6 \times 10^3 \text{ M}^{-1} \text{ cm}^{-1}$  [38]. Measurements were made both with and without 6 M GU.

#### 2.3.4. Quasielastic light scattering

QLS measurements were performed with a 144 channel Langley-Ford model 1097 correlator and a Coherent model Innova 90 Plus argon laser to determine the diffusion coefficients of the oligomers. Instead of reporting the diffusion coefficient, it is customary to characterize the size of the scattering particle by its hydrodynamic radius  $R_h$ . This is the radius of the sphere which would have the same diffusion coefficient as the

particle [39]. To calculate the distribution of hydrodynamic radii of the scattering particles, we used the method described in Braginskaya et al. [40], which was adapted for the analysis of the homodyne correlation function. The conditions of non-negativity and smoothness were superimposed on the size distribution to stabilize this otherwise ill-conditioned problem [41].

Measurements were made at 25°C on the control and oligomer samples at concentrations of 3–5 mg/ml in 100 mM sodium phosphate buffer (pH 7.1) with 0.02% sodium azide.

### 2.3.5. Cation exchange HPLC

CAT-HPLC was performed essentially as described by Siezen et al. [42] using a Bakerbond CBX (5  $\mu$ m) column from Phenomenex (Torrance, CA). The proteins were eluted in 0.02 M Tris acetate containing 0.02% sodium azide, pH 6.5, with a salt gradient of 5–100% 0.5 M sodium acetate for 41 min.

### 2.3.6. Amino acid analysis

Amino acid analyses of the control and oligomeric  $\gamma_{\text{IIIb}}$ -crystallins were performed at the Harvard Microchemistry facility (Cambridge, MA). Samples were analyzed with a 420A amino acid derivatizer (Perkin-Elmer/Applied Biosystems Division, Norwalk, CT) equipped with an online 130A PTC-derivatizer. The data were collected on a CR4A Chromatopac system (Shimadzu Scientific Instruments Inc., Columbia, MD). Solvent A was 50 mM sodium acetate (pH 5.4) and solvent B was 70% acetonitrile in 32 mM sodium acetate (pH 6.1). For most samples, hydrolysis was performed in 6 N HCl at 150°C for 1 h, and a gradient of 7–68% solvent B in 20 min was used for sample elution. However, this procedure failed to resolve the strongly acidic reaction products which elute early in the chromatogram. To enhance the yield of these strongly acidic products, some samples were hydrolysed for 72 h at 110°C, and resolved with a gradient of 5–68% solvent B in 20 min.

### 2.3.7. Electrospray ionization mass spectrometry

ESIMS was used to determine the molecular masses of the native, control and oligomer frac-

tions and to detect the presence of the crosslinker. The  $\gamma_{\text{IIIb}}$ -crystallin samples (at least 10 nmol each) were dialyzed exhaustively into water and were further purified by reversed phase HPLC directly coupled to an electrospray ionization mass spectrometer. Samples were desalted on a C4 microbore column (Vydac, 1  $\times$  50 mm, 5  $\mu$ m; Microtech Scientific, Sunnyvale, CA) using a HPLC binary gradient system (LC-10AD; Shimadzu). Solvent A was water containing 0.05% trifluoroacetic acid and solvent B was acetonitrile containing 0.05% trifluoroacetic acid. A gradient of 30–98% solvent B in 15 min was used for protein elution. The effluent from the HPLC was split, with 10% diverted to a quadrupole electrospray ionization mass spectrometer (Micromass PlatformII, Manchester, UK), and 90% monitored by a UV detector at 220 nm (SPD-10A; Shimadzu). Proteins were delivered to the mass spectrometer in the HPLC effluent. The mass spectrometer was calibrated with horse heart myoglobin over a mass range of 700–1800 Da with a mass accuracy of 2 Da for a 20 kDa protein. Data were processed with MassLynx 2.0 software.

## 2.4. Phase separation measurements

Upon cooling, a homogeneous protein solution may separate into two liquid phases, one rich in protein, the other poor in protein [11]. This liquid–liquid phase separation is analogous to the liquid–liquid phase separation observed in binary mixtures of organic liquids [43]. The coexistence curve marks the boundary between the homogeneous, single phase and the heterogeneous two-phase region. The coexistence curves for the control and oligomer samples were obtained using the method described in detail elsewhere [44]. A brief outline of the procedure is given below.

A protein solution of known concentration is placed in a temperature-controlled water cell and the sample is initially maintained in a single phase state. A laser beam is focused on the sample. The temperature of the sample is then lowered until a reduction in the transmitted intensity is observed. This reduction in intensity is due to the strong light scattering by the domains of protein-rich and protein-poor phases which begin to form.

The temperature of the water bath is then raised until the initial transmitted intensity is recovered i.e. the sample becomes clear again. In this way we obtain both the clouding and clearing temperatures of the solution. Except for concentrations very far from the critical point, the difference between the two temperatures is small (1–2°C). For consistency, the phase separation temperature is taken to be the average of these two temperatures [44].

We determined the complete coexistence curve for the  $\gamma_{IIIb}$  dimers and a partial coexistence curve for the trimer. We wish to emphasize that to obtain a reliable coexistence curve no less than 50 mg of protein are needed [30]. The crosslinking reaction we have used allows us to produce large quantities of dimer, but smaller amounts of the trimer. The coexistence curve for the native, monomer  $\gamma_{IIIb}$  has been published earlier from this laboratory [19]. In this report we also present partial coexistence curves for the pr-monomer and  $n$ -mer fractions.

### 3. Results

#### 3.1. Physical characterization of oligomers

The sizes of the oligomers formed were characterized by SDS/PAGE, SX-HPLC, QLS, and ES-IMS.

The SDS/PAGE results (Fig. 3) show that the major dimer (lanes 5 and 6) and trimer (lanes 8 and 9) bands have molecular weights of  $\approx 41$  kDa and  $\approx 62$  kDa, respectively. These molecular weights are consistent with the known, native monomer molecular weight of  $\approx 21$  kDa [45]. Tetramers ( $\approx 85$  kDa) and pentamers ( $\approx 97$  kDa) were seen in the high  $n$ -mer fraction (lane 10). SDS/PAGE experiments following a 4-h incubation with 100 mM DTT (data not shown) gave results almost identical to those presented in Fig. 3.

We note that, as expected, the control sample (lane 3) appears identical to the native sample (lane 2). The native is a  $\gamma_{IIIb}$ -crystallin sample that was not incubated in parallel with the control or oligomer samples, but set aside at 4°C and pH 4.8 (see Section 2.1).

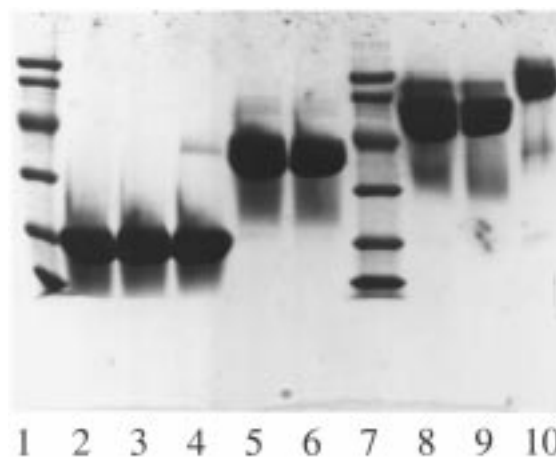


Fig. 3. SDS/PAGE of the oligomers of  $\gamma_{IIIb}$  without DTT. Lanes: 1 and 7, molecular mass markers (from bottom to top) are 14.4, 21.5, 31.0, 45.0, 66.2 and 97.4 kDa; lane 2, native  $\gamma_{IIIb}$ ; lane 3, control  $\gamma_{IIIb}$ ; lane 4, monomer fraction after crosslinking; lanes 5 and 6, dimer fraction; lanes 8 and 9, trimer fraction; lane 10,  $n$ -mer mixture.

The SX-HPLC elution times for the various oligomers were consistent with the molecular weights found by SDS/PAGE. Over a period of 1 week there was no measurable dissociation of the protein oligomers as determined by SX-HPLC.

In Fig. 4 we show the normalized scattering intensity plotted against the apparent hydrodynamic radius  $R_h$  as obtained by QLS for the control and oligomer samples. The height of each bar gives the fraction of the light scattering intensity associated with each range of  $R_h$ . The results for the  $\gamma_{IIIb}$  oligomers are shown in Fig. 4A–D: control monomer (A); dimer (B); trimer (C); and  $n$ -mer mixture (D). The average hydrodynamic radius  $\langle R_h \rangle$  increases with aggregation number as expected [46].

In Fig. 4E and F we present the results for the  $\gamma_{II}$  monomer and for  $\gamma_{III}$ , respectively, adapted from Pande et al. [23]. It is evident that the  $\langle R_h \rangle$  values for the native  $\gamma_{II}$  and ‘dimer’  $\gamma_{III}$  are larger than the corresponding sizes for the native and dimeric  $\gamma_{IIIb}$ . These results will be discussed in Section 4 where we compare our model system with that of  $\gamma_{II}$ .

Our ESIMS data for the native and control  $\gamma_{IIIb}$  monomers give a molecular weight of 20 747

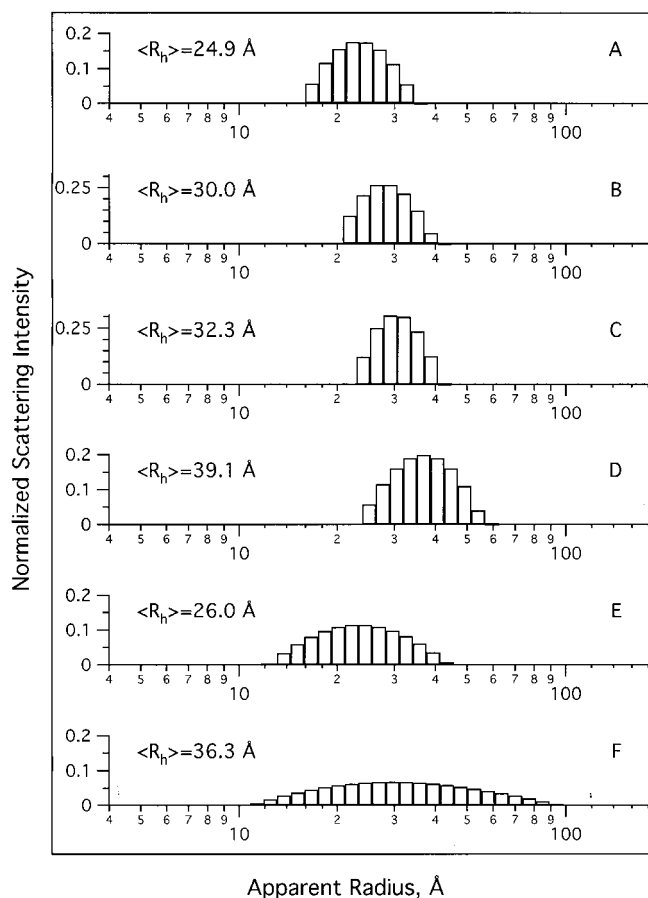


Fig. 4. QLS data for  $\gamma_{IIIb}$ - and  $\gamma_{II}$ -crystallins. Normalized scattering intensity is plotted against apparent  $R_h$ . (A)  $\gamma_{IIIb}$  control monomer; (B)  $\gamma_{IIIb}$  dimer; (C)  $\gamma_{IIIb}$  trimer; (D)  $\gamma_{IIIb}$   $n$ -mer mixture; (E)  $\gamma_{II}$  monomer (from Ref. [23]); (F)  $\gamma_{IIIH}$  (from Ref. [23]).

Da, which is in good agreement with the published value of 20749 Da (calculated from the cDNA sequence determined by Hay et al. [47] and also obtained by Kilby et al. [48] using mass spectrometry). The results for the pr-monomer and dimer are shown in Fig. 5A and B, respectively. For the pr-monomer (Fig. 5A), the mass of  $M_r$  20746 corresponds to one protein molecule without a linker, while the mass of  $M_r$  21024 corresponds to one protein molecule and one linker. For the dimer (Fig. 5B), the mass of  $M_r$  41768 corresponds to two protein molecules and one linker, while the mass of  $M_r$  42042 corresponds to two protein molecules and two linkers. We see a similar pattern for the higher oligomers as well: one large peak accompanied by another

smaller peak with the same number of protein molecules, but with one extra crosslinker present. The molecular weights of all of the oligomers with the crosslinkers are consistent with the molecular weight of the control monomer and with the calculated molecular weight of 276.3 Da for the crosslinker BMH. Thus our ESIMS results confirm that BMH has reacted with the protein to form oligomers as expected.

### 3.2. Chemical characterization of oligomers

We have used the DTNB assay and amino acid analysis to check if the crosslinking reaction between BMH and cysteine residues on the protein had indeed taken place. The results of our

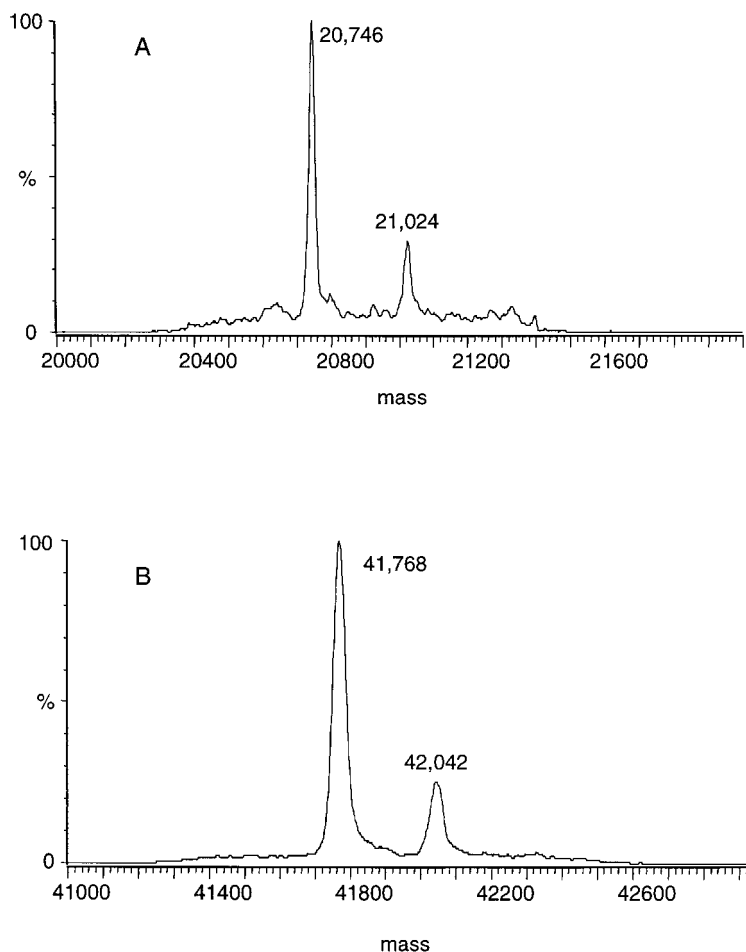


Fig. 5. ESIMS results for the  $\gamma_{IIIb}$  oligomers: (A) pr-monomer; (B) dimer. (A) The molecular weight of  $M_r$  20 746 corresponds to one protein molecule with no crosslinker. The molecular weight of  $M_r$  21 024 corresponds to one protein molecule with one crosslinker; (B) the molecular weight of  $M_r$  41 768 corresponds to two protein molecules with one crosslinker. The molecular weight of  $M_r$  42 042 corresponds to two protein molecules with two crosslinkers.

thiol assay are shown in Table 1. For each protein species in the table, we present the average number of unreacted thiols per monomeric unit both in the absence and in the presence of GU. As expected, for any given oligomer there are fewer free thiols for the non-denatured protein (without 6 M GU) than for the denatured protein. However, we find that the number of free thiols for the denatured native protein (3.5) is smaller than the five free thiols expected from the cDNA sequence [47]. Therefore, even in the denatured state, it appears that not all the thiol groups are available for reaction with DTNB. This may be

due to an intramolecular disulphide crosslink present in the native state of  $\gamma_{IIIb}$ -crystallin, although such a disulphide crosslink has not been observed in the three dimensional X-ray crystal structure of the protein [49]. The control and native samples are practically identical, while each protein in the dimer has one free thiol fewer than in the native monomeric state. The pr-monomer has on average 0.3 free thiols fewer than the control protein, which is consistent with our ESIMS result that approximately one quarter of the pr-monomers contain a crosslinker (Fig. 5A).

We have performed the crosslinking reaction

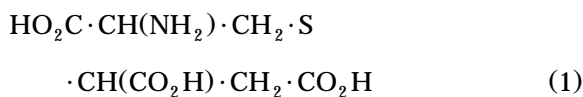
Table 1  
Number of free thiols per monomeric unit as determined by the DTNB assay [38]

	Native	Control	Dimer	pr-Monomer
Without 6 M GU	1.9	1.8	0.9	1.5
With 6 M GU	3.5	3.3	2.5	3.0

Each result represents an average of two measurements. The precision of the results is  $\pm 0.1$  free thiol. The total number of thiols in the native and control protein is five [47].

under conditions where the maleimide group is specific towards the thiol groups of the cysteine residues [34]. However, it has been noted that reactions with free amino groups and the imidazole group of histidine are also possible [50]. In the case of  $\gamma_{\text{IIIb}}$ , BMH appears to target only the thiol group of the cysteines. Amino acid analysis of the oligomers shows no significant difference in the number of glycine, lysine and histidine residues between the oligomers and the control protein. This indicates that the  $\alpha$ -amino group of the N-terminal glycine, the  $\epsilon$ -amino groups of the two lysine residues and the imidazole groups of the seven histidine residues are unmodified by the reaction with BMH.

Amino acid analysis also confirmed that BMH had reacted with the cysteine thiols. The hydrolysis product of the maleimide-cysteine crosslink should be observable in amino acid analysis [50]. This product, *S*-(1,2-dicarboxyethyl)-L-cysteine,



is strongly acidic and should elute very early from the reversed phase HPLC amino acid analysis column. We therefore conducted amino acid analyses under conditions which increase the yield and resolution of *S*-(1,2-dicarboxyethyl)-L-cysteine (see Section 2.3.6). Under these analysis conditions, we observed large peaks eluting at very early times for the dimer, trimer and *n*-mer samples. Moreover, these peaks eluted at the same retention times as samples of cysteine which were reacted with BMH under conditions identical to the protein-BMH crosslinking reactions.

The early eluting, acidic peaks were absent in the control and native  $\gamma_{\text{IIIb}}$  samples. The detection of *S*-(1,2-dicarboxyethyl)-L-cysteine in the oligomer samples confirms that BMH did react with the cysteine residues.

### 3.3. Coexistence curves of oligomers

In Fig. 6 we present the coexistence curves for oligomers of  $\gamma_{\text{IIIb}}$ -crystallin in 100 mM sodium phosphate solution (pH 7.1). We show our results for the phase separation temperature as a function of protein volume fraction for the following systems:  $\gamma_{\text{IIIb}}$  pr-monomers (solid bowties), the  $\gamma_{\text{IIIb}}$  dimers (solid circles) and the  $\gamma_{\text{IIIb}}$  trimers (solid triangles). The monomer  $\gamma_{\text{IIIb}}$  (taken from Ref. [19]) is also shown (open squares) together with our control sample (open circles). As can be seen in the figure, we find excellent agreement between our control sample and the results of Broide et al. [19].

The solid lines in the figure are fits of the coexistence curves to the function [51]

$$\left| \frac{\phi - \phi_c}{\phi_c} \right| = A \left( 1 - \frac{T}{T_c} \right)^\beta \quad (2)$$

where  $\phi$  is the volume fraction of protein in solution,  $\phi_c$  is the critical volume fraction,  $A$  is a parameter that characterizes the width of the coexistence curve,  $T$  is the temperature (in Kelvin),  $T_c$  is the critical temperature and  $\beta = 0.325$  (the exponent for the three-dimensional Ising model [52]). In Table 2 we list the values of the parameters  $\phi_c$ ,  $T_c$  and  $A$  for the native monomer and for the dimer which correspond to the solid line fits in the figure.

We observe that the dimer has a lower critical volume fraction, a higher critical temperature and a narrower coexistence curve than the monomer. Since we could only obtain a partial coexistence curve for the trimers, we could not determine the values of  $\phi_c$  and  $A$ . We estimate that the critical temperature of the trimer is  $T_c = 317$  K, which is higher than that of the dimer ( $T_c = 304.7$  K) and the control monomer ( $T_c = 278.4$  K). More gener-

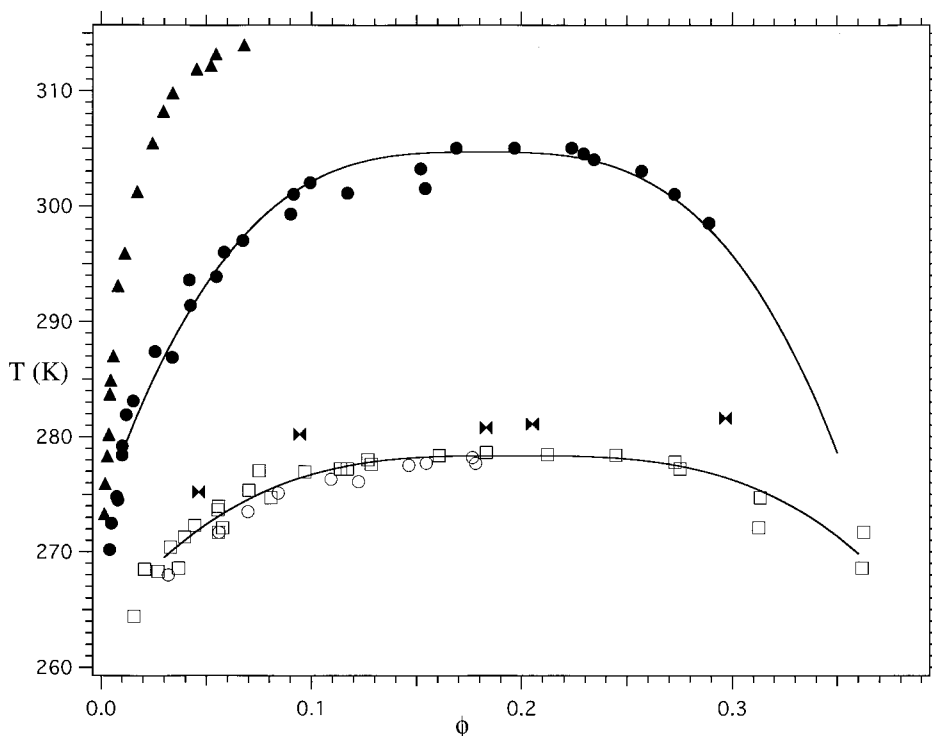


Fig. 6. Coexistence curves for the oligomers of  $\gamma_{IIIb}$ -crystallin in 0.1 M sodium phosphate (pH 7.1). Native monomers, from Ref. [19] (open squares); control monomers, this report (open circles); pr-monomers (solid bowties); dimers (solid circles); trimers (solid triangles). The solid lines are fits to Eq. (2).

Table 2  
Coexistence curve parameters for the  $\gamma_{IIIb}$  monomer and dimer

Oligomer	$\phi_c$	$T_c$ (K)	$A$
Monomer	$0.20 \pm 0.01$	$278.4 \pm 0.2$	$2.6 \pm 0.1$
Dimer	$0.18 \pm 0.01$	$304.7 \pm 0.5$	$2.1 \pm 0.1$

Here we present the critical volume fraction  $\phi_c$ , the critical temperature  $T_c$  and the width of the coexistence curve  $A$  (see also Eq. (2) in the text).

ally, we see from Fig. 6 that at a fixed concentration the phase separation temperature markedly increases with the size of the oligomer.

Another significant observation is that the critical temperature of the pr-monomer (solid bowties) is  $\sim 281$  K, which is 3 K higher than that of the control protein. This change is perhaps due to the nearly 25% of the pr-monomer which contains a crosslinker (Fig. 5A). In previous studies on phase separation in mixtures of two proteins with dif-

ferent critical temperatures [44,53], we observed experimentally that for many mixtures the critical temperature increases approximately linearly with the proportion of the higher  $T_c$  component. If we assume that such a linear approximation holds for the pr-monomer, then we would expect the critical temperature of 100% of the pr-monomer with one crosslinker to be  $\sim 12$  K higher than the native monomer.

#### 4. Discussion

Our physical characterization of the dimer, trimer and higher  $n$ -mers shows that they are stable, covalently bound complexes of monomeric  $\gamma_{IIIb}$ -crystallin. Our chemical analyses strongly support the proposed linkage of the dimer shown in Fig. 1. Our work also suggests that the larger oligomers are connected in similar fashion i.e. through the bonding of BMH to the cysteine residues.

A significant feature of our crosslinking method is the production of large quantities of dimeric [54] and oligomeric species. Production of large quantities of dimer are important not only for the phase separation studies presented here, but also in other biochemical and spectroscopic work. A typical example is the study of enzymes for which enzymatic activity is enhanced through the formation of oligomers [55]. Furthermore, techniques such as NMR and Raman spectroscopies require millimolar amounts of the protein species being characterized [56,57]. We therefore propose a reaction scheme which explains the high yields of dimer obtained in our crosslinking reaction.

The predominance of the dimer over other oligomers in the reaction (see Fig. 2) suggests that one thiol group is much more reactive than the rest. This has been demonstrated for the reaction of  $\gamma_{\text{IIIb}}$  with glutathione [27]. The existence of one most reactive thiol is also consistent with the three dimensional X-ray crystal structure of  $\gamma_{\text{IIIb}}$ , which shows that only one of the five thiol groups present in the protein has significant surface accessibility ( $\sim 7 \text{ \AA}^2$ ) [49].

The formation of dimers is a two step process. First, a monomer must react with the crosslinker. Second, a monomer containing a crosslinker must react with a monomer lacking a crosslinker (a 'free' monomer). In a reaction such as ours, which is terminated before any of the reactants is exhausted, the outcome is determined by the ratio of the rates of the above two steps. If the rate of the first step is very large compared to that of the second, most of the monomers will have a crosslinker attached to them. Consequently, there will be few free monomers available and hence few dimers will be formed [58]. On the other hand, if the rate of the second step is larger than that of the first, then once a monomer containing a crosslinker is produced, it promptly reacts with a free monomer to form a dimer. In this case, as the reactions proceed, the fraction of the monomers which have a crosslinker will be small. This is indeed observed in our ESIMS for the pr-monomer (see Fig. 5A; only 25% of the pr-monomer has a linker attached). Thus, as expected from the low solubility of BMH, the reac-

tion between  $\gamma_{\text{IIIb}}$  and the crosslinker is the rate limiting step.

The majority of the dimers produced are held together by a crosslink which connects the most reactive or primary thiol on one protein to the most reactive thiol on another. These dimers are relatively unreactive, for the sites on the dimers which are available for further reaction are the less reactive, remaining thiols. Dimers which possess an available most reactive thiol are rare since such dimers are formed by an intermolecular crosslink between a reactive thiol on one protein and a secondary thiol on another. Thus, regardless of the kinetic pathway, the trimers and higher oligomers are expected to form very slowly because the existence of these oligomers necessarily involves the less reactive secondary thiols. Therefore, the dimer species is expected to dominate the distribution of oligomers, which is consistent with our observations (Fig. 2).

In the scheme proposed above, the high yield of the dimer is due to two properties of the system: a single most reactive crosslinking site and a slow reaction rate of the crosslinker with the monomer (as compared to the rate of dimerization). These two criteria can be useful in optimizing the yield of dimer for other protein-crosslinker systems as well. Group-specific crosslinkers should be used instead of non-specific ones such as glutaraldehyde [59]. For fast-reacting, specific crosslinkers, the effect of a slow crosslinking reaction can be obtained by the gradual release of the crosslinker so that at each moment its concentration is small compared to the concentration of free monomers.

One important application of our model system is in cataract research, where we wish to understand the aggregation and phase separation behavior of the  $\gamma$ -crystallins. In Fig. 7 we compare the coexistence curves for the oligomers of  $\gamma_{\text{IIIb}}$ -crystallin with those of  $\gamma_{\text{II}}$ -crystallin. The native  $\gamma_{\text{IIIb}}$  and  $\gamma_{\text{II}}$  monomers are shown as open squares and open triangles, respectively. The solid symbols represent our results for the  $\gamma_{\text{IIIb}}$  oligomers: dimers (solid circles), trimers (solid triangles) and a mixture of higher  $n$ -mers (solid squares). We estimated (from our Superdex 75

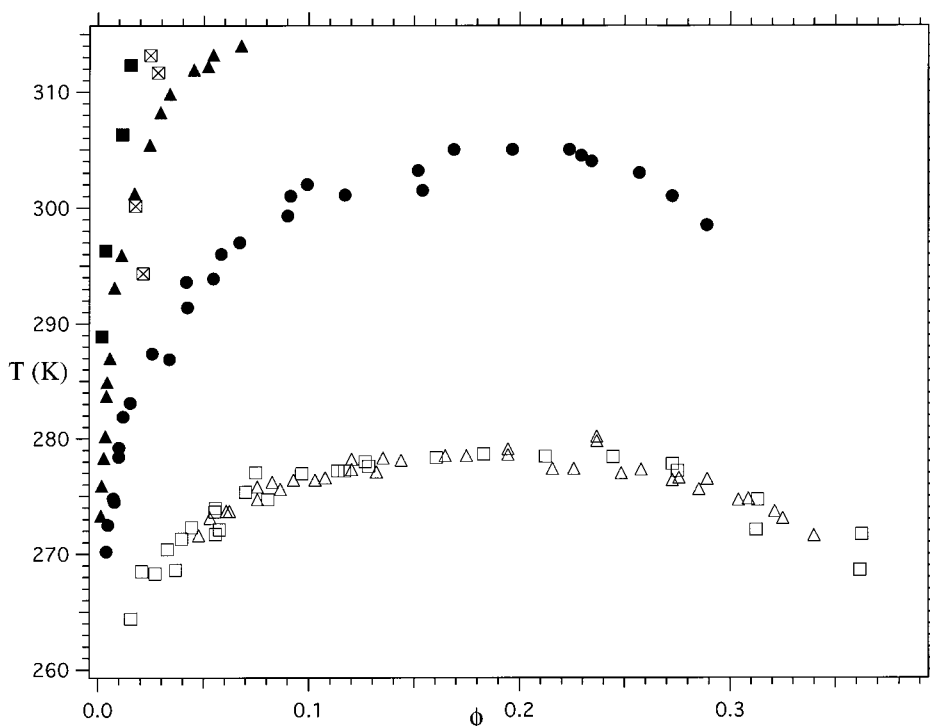


Fig. 7. Comparison of the coexistence curves for  $\gamma_{\text{IIB}}$  and  $\gamma_{\text{II}}$  oligomers. Native  $\gamma_{\text{IIB}}$  and  $\gamma_{\text{II}}$  monomers, from Ref. [19] (open squares and open triangles, respectively);  $\gamma_{\text{IIB}}$  dimers (solid circles);  $\gamma_{\text{IIB}}$  trimers (solid triangles);  $\gamma_{\text{IIB}}$   $n$ -mers (solid squares);  $\gamma_{\text{IIH}}$  from Ref. [23] (crossed squares).

separation — see Section 2.2) that the  $n$ -mer mixtures contained  $\sim 10\%$  trimers,  $70\%$  tetramers and  $20\%$  pentamers. The crossed squares are the results for the partial coexistence curve of  $\gamma_{\text{IIH}}$  obtained by Pande et al. [23].

We see from this figure, that although the coexistence curves of the  $\gamma_{\text{IIB}}$  and  $\gamma_{\text{II}}$  monomers are practically the same, the partial coexistence curve of  $\gamma_{\text{IIB}}$  is very different from that of the  $\gamma_{\text{IIB}}$  dimer; it resembles more closely the partial coexistence curve of the  $\gamma_{\text{IIB}}$   $n$ -mers. It is possible that some of the differences in phase behavior arise from the different chemical nature of the protein crosslink, since the  $\gamma_{\text{IIB}}$  dimer contains a long, extrinsic crosslinker while  $\gamma_{\text{IIH}}$  does not. However, a comparison of the  $\gamma_{\text{IIB}}$  and  $\gamma_{\text{II}}$  QLS data (Fig. 4B, F) reveals that  $\gamma_{\text{IIH}}$  contains a significant fraction of particles larger than dimers. Thus, it is the  $\gamma_{\text{IIB}}$   $n$ -mer mixture, and not the  $\gamma_{\text{IIB}}$  dimers, which most closely resembles  $\gamma_{\text{IIH}}$

in the distribution of particle sizes. These observations suggest that the loosely associated oligomers make a significant contribution to the high phase separation temperature of  $\gamma_{\text{IIH}}$  and that this high temperature is not due solely to the covalent dimer fraction, as had been previously suggested [24]. However, the  $\gamma_{\text{IIH}}$  model does suggest that the aggregation of the lens proteins may cause the phase separation temperature to increase in vivo as well as in vitro, especially since aggregation in vivo will most likely proceed beyond the dimer stage:  $\gamma$ -crystallin aggregates, containing both dimers with intermolecular disulfide bridges and physically associated oligomers, have been isolated from cataractous lenses [16,21]. Furthermore, it has been observed that the phase separation temperature of rabbit lenses increases after irradiation by X-rays [60] and that under the same conditions high molecular weight aggregates also form [61].

It is clear from the above discussion that aggregates can strongly affect the phase behavior of protein solutions by changing the location of the phase boundaries. In fact, the similarity between the phase behavior of the naturally occurring species  $\gamma_{\text{IIIH}}$  and the artificial  $\gamma_{\text{IIIb}}$   $n$ -mers indicates that for phase separation the details of the surface properties are less important than the purely steric effects of oligomerization. However, further work must be carried out to determine whether the effect of oligomerization on phase separation observed here is applicable to a larger group of proteins. The study of different phase separating proteins will be important not only to understand a variety of protein condensation diseases [4], but also to examine other phenomena, such as crystallization, which involve high concentrations of protein. Our findings suggest that aggregates may allow liquid–liquid phase separation to occur at higher temperatures and compete with the crystallization process.

The experimental methods presented above allow large quantities of pure and stable oligomers to be produced. With these methods we will be able to form controllably a wide variety of dimers and higher oligomers by merely changing the length of the crosslinker spacer arm or the identity of the crosslinker. We will then be able to test more stringently the extent to which the effects of oligomerization are independent of the chemical nature of the oligomers. We believe that the model system we have developed will facilitate systematic investigations of the effect of aggregation on the thermodynamic behavior of globular protein solutions.

### Acknowledgements

We thank Drs. Ajay Pande and George Thurston for helpful discussions and critical comments. This work was supported by grants EY05127 (G.B.B.), EY10535 (J.P.) and EY07609 (J.B.S.) from the National Eye Institute of the National Institutes of Health.

### References

[1] F.J. Reithel, in: C.B. Anfinsen Jr., M.L. Anson, J.T.

- Edsall (Eds.), *Advances in Protein Chemistry*, vol. 18, Academic Press, New York, 1963, p. 123.
- [2] F.A.O. Marston, D.L. Hartley, *Methods Enzymol.* 182 (1990) 264.
- [3] V.H.K. Li, J.R. Robinson, V.H.L. Lee, in: J.R. Robinson, V.H.L. Lee (Eds.), *Controlled Drug Delivery: Fundamentals and Applications*, 2nd ed., Marcel Dekker, New York, 1987, Chapter 1.
- [4] G.B. Benedek, *Invest. Ophthalmol. Vis. Sci.* 38 (1997) 1911.
- [5] D.F. Waugh, in: M.L. Anson, K. Bailey, J.T. Edsall (Eds.), *Advances in Protein Chemistry*, vol. 9, Academic Press, New York, 1954, p. 325.
- [6] D.E. Brooks, K.A. Sharp, D. Fisher, in: H. Walter, D.E. Brooks, D. Fisher (Eds.), *Partitioning in Aqueous Two-Phase Systems: Theory, Methods, Uses, and Applications to Biotechnology*, Academic Press, New York, 1985, Chapter 2.
- [7] A. George, Y. Chiang, B. Guo, A. Arabshahi, Z. Cai, W.W. Wilson, *Methods Enzymol.* 276 (1997) 100.
- [8] A. McPherson, *Preparation and Analysis of Protein Crystals*, John Wiley, New York, 1982, Chapters 3 and 4.
- [9] P.-Å. Albertsson, *Partition of Cell Particles and Macromolecules*, 3rd ed., John Wiley, New York, 1986, Chapter 9.
- [10] A.H. Palmer, *J. Biol. Chem.* 104 (1934) 359.
- [11] M.P. Tombs, B.G. Newsom, P. Wilding, *Int. J. Peptide Protein Res.* 6 (1974) 253.
- [12] V.B. Tolstoguzov, *Food Hydrocolloids* 2 (1988) 339.
- [13] V. Mikol, E. Hirsch, R. Giegé, *J. Mol. Biol.* 213 (1990) 187.
- [14] F. Rosenberger, P.G. Velikov, M. Muschol, B.R. Thomas, *J. Cryst. Growth* 168 (1996) 1.
- [15] D.E. Kuehner, C. Heyer, C. Rämisch, U.M. Fornefeld, H.W. Blanch, J.M. Prausnitz, *Biophys. J.* 73 (1997) 3211.
- [16] J.J. Harding, M.J.C. Crabbe, in: H. Davson (Ed.), *The Eye*, 3rd ed., vol. 1b, Academic Press, New York, 1984, Chapter 3.
- [17] J.A. Thomson, P. Schurtenberger, G.M. Thurston, G.B. Benedek, *Proc. Natl. Acad. Sci. USA* 84 (1987) 7079.
- [18] P. Schurtenberger, R.A. Chamberlin, G.M. Thurston, J.A. Thomson, G.B. Benedek, *Phys. Rev. Lett.* 63 (1989) 2064.
- [19] M.L. Broide, C.R. Berland, J. Pande, O.O. Ogun, G.B. Benedek, *Proc. Natl. Acad. Sci. USA* 88 (1991) 5660.
- [20] C.R. Berland, G.M. Thurston, M. Kondo, M.L. Broide, J. Pande, O. Ogun, G.B. Benedek, *Proc. Natl. Acad. Sci. USA* 89 (1992) 1214.
- [21] A. Spector, in: J. Nugent, J. Whelan (Eds.), *Human Cataract Formation*, Ciba Foundation Symposium, vol. 106, Pitman, London, 1984, p. 48.
- [22] R.J. Siezen, M.R. Fisch, C. Slingsby, G.B. Benedek, *Proc. Natl. Acad. Sci. USA* 82 (1985) 1701.
- [23] J. Pande, A. Lomakin, B. Fine, O. Ogun, I. Sokolinski, G. Benedek, *Proc. Natl. Acad. Sci. USA* 92 (1995) 1067.
- [24] G. Friberg, J. Pande, O. Ogun, G.B. Benedek, *Curr. Eye Res.* 15 (1996) 1182.

- [25] J. Pande, C. Berland, M. Broide, O. Ogun, J. Melhuish, G. Benedek, *Proc. Natl. Acad. Sci. USA* 88 (1991) 4916.
- [26] J. Pande, O. Ogun, C. Nath, G. Benedek, *Exp. Eye Res.* 57 (1993) 257.
- [27] C. Slingsby, L. Miller, *Biochem. J.* 230 (1985) 143.
- [28] N.-T. Yu, D.C. DeNagel, C. Slingsby, *Exp. Eye Res.* 48 (1989) 399.
- [29] H.A. Sober, *Handbook of Biochemistry: Selected Data for Molecular Biology*, 2nd ed., The Chemical Rubber Company, Cleveland, 1970, pp. C10–C23.
- [30] C. Liu, Ph.D. Thesis, Massachusetts Institute of Technology, 1995.
- [31] F. Yi, B.M. Denker, E.J. Neer, *J. Biol. Chem.* 266 (1991) 3900.
- [32] L.L. Chen, J.J. Rosa, S. Turner, R.B. Pepinsky, *J. Biol. Chem.* 266 (1991) 18237.
- [33] R.B. Pepinsky, L.L. Chen, W. Meier, B.P. Wallner, *J. Biol. Chem.* 266 (1991) 18244.
- [34] S.S. Wong, *Chemistry of Protein Conjugation and Cross-linking*, CRC Press, Boca Raton, 1991, p. 108.
- [35] F. Wold, *Methods Enzymol.* 25 (1972) 623.
- [36] U.K. Laemmli, *Nature* 227 (1971) 680.
- [37] K. Weber, M. Osborn, *J. Biol. Chem.* 244 (1969) 4406.
- [38] R.J.W. Truscott, F. Martin, *Exp. Eye Res.* 49 (1989) 927.
- [39] K.S. Schmitz, *An Introduction to Dynamic Light Scattering by Macromolecules*, Academic Press, New York, 1990, pp. 50–52.
- [40] T.G. Braginskaya, P.D. Dobichin, M.A. Ivanova, V.V. Kublin, A.V. Lomakin, V.A. Noskin, G.E. Shmelev, S.P. Tolpina, *Phys. Scripta* 28 (1983) 73.
- [41] E.R. Pike, in: S.H. Chen, B. Chu, R. Nossal (Eds.), *Scattering Techniques Applied to Supramolecular and Nonequilibrium Systems*, Plenum, New York, 1981, p. 179.
- [42] R.J. Siezen, E.D. Kaplan, R.D. Anello, *Biochem. Biophys. Res. Commun.* 127 (1985) 153.
- [43] A.W. Francis, *Liquid–Liquid Equilibria*, John Wiley, New York, 1963, Chapter 2.
- [44] C. Liu, N. Asherie, A. Lomakin, J. Pande, O. Ogun, G.B. Benedek, *Proc. Natl. Acad. Sci. USA* 93 (1996) 377.
- [45] P.F. Lindley, M.E. Narebor, L.J. Summers, G.J. Wistow, in: H. Maisel (Ed.), *The Ocular Lens: Structure, Function, and Pathology*, Marcel Dekker, New York, 1985, p. 123.
- [46] J.G. de la Torre, V.A. Bloomfield, *Q. Rev. Biophys.* 14 (1981) 81.
- [47] R.E. Hay, U.P. Andley, J.M. Petrash, *Exp. Eye Res.* 58 (1994) 573.
- [48] G.W. Kilby, R.J.W. Truscott, J.A. Aquilina, M.A. Sheil, M.L. Riley, J.J. Harding, *Eur. Mass. Spectrom.* 1 (1995) 203.
- [49] Yu.N. Chirgadze, H.P.C. Driessen, G. Wright, C. Slingsby, R.E. Hay, P.F. Lindley, *Acta Cryst. D52* (1996) 712.
- [50] D.G. Smyth, O.O. Blumenfeld, W. Konisberg, *Biochem. J.* 91 (1964) 589.
- [51] H.E. Stanley, *Introduction to Phase Transitions and Critical Phenomena*, Oxford University Press, New York, 1971, p. 42.
- [52] P.K. Pathria, *Statistical Mechanics*, 2nd ed., Butterworth-Heinemann, Oxford, 1996, pp. 405–407.
- [53] C. Liu, A. Lomakin, G.M. Thurston, D. Hayden, A. Pande, J. Pande, O. Ogun, N. Asherie, G.B. Benedek, *J. Phys. Chem.* 99 (1995) 454.
- [54] V.H. Zahn, L. Lumper, *Hoppe-Seyler's Z. Physiol. Chem.* 349 (1968) 485.
- [55] S. Sorrentino, G.I. Yakovlev, M. Libonati, *Eur. J. Biochem.* 124 (1982) 183.
- [56] B.W. Bangerter, in: J.A. Glasel, M.P. Deutscher (Eds.), *Introduction to Biophysical Methods for Protein and Nucleic Acid Research*, Academic Press, New York, 1995, pp. 360–361.
- [57] T. Miura, G.J. Thomas Jr., in: J.A. Glasel, M.P. Deutscher (Eds.), *Introduction to Biophysical Methods for Protein and Nucleic Acid Research*, Academic Press, New York, 1995, pp. 293–295.
- [58] P.M. Conn, D.C. Rogers, R. McNeil, *Endocrinology* 111 (1982) 335.
- [59] F. Wang, J. Hayter, L.J. Wilson, *Acta Cryst. D52* (1996) 901.
- [60] J.I. Clark, F.J. Giblin, V.N. Reddy, G.B. Benedek, *Invest. Ophthalmol. Vis. Sci.* 22 (1982) 186.
- [61] F.J. Gilbin, B. Chakrapni, V.N. Reddy, *Exp. Eye Res.* 26 (1978) 507.